第 43 卷 第 18 期/2023 年 9 月/光学学报 特邀论文

光学学报

基于虚像相位阵列光谱仪的宽带高分辨率 CO_2 吸收光谱测量技术研究

周昊[1,2]，赵卫雄[1,2*]，吕丙选[1,2]，崔卫华[1]，方波[1]，杨娜娜[1]，张为俊[1,2]

[1]中国科学院合肥物质科学研究院安徽光学精密机械研究所，安徽 合肥 230031；

[2]中国科学技术大学，安徽 合肥 230036

摘要 为了使光谱仪能同时兼顾宽吸收光谱范围和高光谱分辨率两种特性，搭建了一台近红外虚像相位阵列光谱仪，单帧谱宽约为 25 nm(140 cm^{-1})，光谱分辨率为 4.5 pm(0.024 cm^{-1})，结合改进的旋转光栅结构，实现了 1.26～1.50 μm 的宽光谱检测。使用超连续光源及光学吸收多通池，在 1.43～1.45 μm 处，以 CO_2 为例开展了宽带高分辨光谱测量技术研究，使用图像增强算法提高了弱吸收的光谱提取精度，考虑光谱仪的仪器展宽进而提升了气体参数反演准确度。实测光谱与理论光谱的对比结果验证了系统测量的准确性与可靠性。

关键词 虚像相位阵列光谱仪；宽带吸收光谱；高分辨率；CO_2 探测

中图分类号 O439 **文献标志码** A **DOI**：10.3788/AOS230905

1 引 言

通过光谱信息能够精准识别物质种类[1]、测量反演物质浓度及温度等信息[2-6]，该技术在大气痕量探测[7]、工业监测[8]、精密测量[9]及众多基础物理和化学[10-11]等研究领域有广泛应用。相较于窄带可调谐吸收光谱技术，宽光谱允许同时检测多种物质[1]，使单一设备具备多种用途[12]。随着超连续光源[13]、光学频率梳[14]等先进宽带激光光源的发展，结合宽带激光光源和光谱仪的宽带吸收光谱技术受到越来越多的关注[15]。然而受到光谱仪分辨率限制，光谱高精细结构反演依然存在挑战。

在宽带光谱测量中，最常用的光谱检测仪器为光栅光谱仪。光栅的周期性结构调制入射光的幅值与相位，使出射光在焦平面发生干涉从而将不同波长光分离。结合线阵探测器可快速获取数百 nm 波长范围的宽光谱信息。然而受限于单位面积的刻线数目，光栅光谱仪的光谱分辨率一般在 nm、亚 nm 量级[16]，难以用于更高分辨光谱测量。通过使用刻线密度更低、闪耀角度更大的中阶梯光栅可以实现数百至数十 pm 的光谱分辨率[17]，然而其分辨率与光栅尺寸相关，实现 pm 级别的精细光谱测量仍然极具挑战[18]。

虚像相位阵列(VIPA)是 Shirasaki[19]在 1996 提出的一种新型色散器件，拥有比中阶梯光栅更高的色散能力，其外形类似于 Fabry-Perot 标准具。VIPA 器件结合光栅等色散元件组成的交叉色散光谱仪，通常称为 VIPA 光谱仪，单帧能够实现数十 nm 波长覆盖范围及 pm 量级的光谱分辨率[20]。目前 VIPA 光谱仪已被广泛应用于气体吸收检测领域[19-22]。2007 年 Diddams 等[21]使用 VIPA 光谱仪结合光学频率梳测量了 633 nm 附近碘分子的宽带吸收光谱。2016 年 Klose 等[3]使用 VIPA 光谱仪测量了近红外 2 μm 处 CO_2 吸收光谱，实现气体温度的反演。2020 年 Bailey 等[23]使用 VIPA 光谱仪测量了中红外 4.5 μm 附近 N_2O 吸收光谱，实现 N 同位素的精确测量。

VIPA 光谱仪应用于气体吸收检测时，数据处理算法的准确性是气体参数反演精度的关键。目前常用的算法[1,3]使用气体吸收信息标定 VIPA 光谱图像，进而实现气体参数反演。此类方法虽具有装置简单、标定简便的优点，但忽略了光谱仪的仪器展宽，在应用于高精细光谱(气体展宽与仪器展宽相当)反演时，存在较大的误差，因此此类算法需考虑仪器展宽参数[23]。

本文报道了一台近红外 VIPA 光谱仪，单帧谱宽约为 25 nm(140 cm^{-1})，光谱分辨率为 4.5 pm(0.024 cm^{-1})。在结构上采用一体化设计，添加了光栅旋转结构，将光谱仪的实际检测范围扩展为 1.26～

收稿日期：2023-05-04；**修回日期**：2023-06-02；**录用日期**：2023-06-15；**网络首发日期**：2023-06-25

基金项目：国家自然科学基金(42022051，U21A2028)、中国科学院青年创新促进会(Y202089)、中国科学院合肥物质科学研究院院长基金(YZJJ202101)

通信作者：*wxzhao@aiofm.ac.cn

1.50 μm，并改进了调节结构，在简化光谱仪的同时有效控制了系统的离轴像差。结合超连续光源和Chernin型光学吸收多通池，对1.43～1.45 μm波段的CO_2高分辨吸收光谱开展了测量研究。在数据处理算法中添加了图像增强算法，提升弱信号的提取精度。同时，考虑了仪器展宽，提高了气体参数反演准确度。最后评估了系统的性能指标，验证了VIPA光谱仪能够用于pm分辨吸收光谱的准确测量，具有宽带、高光谱分辨率的优点。

2　原 理

2.1　VIPA光谱仪原理

正交色散结构的VIPA光谱仪如图1(a)所示。光谱仪主要由柱面镜、VIPA元件、闪耀光栅、成像镜和面阵探测器等组成。VIPA色散元件是一块双面镀膜的平行平板，其入射面除入射窗口区外镀有反射率约为100%的反射膜，出射面镀有约95%的部分反射膜[19]。入射光在VIPA元件前后表面来回反射且每次有部分光从后表面出射，相邻出射光间存在稳定的光程差，从而在焦平面发生干涉，实现探测光的色散分光，其理论光谱分辨率与自由光谱范围(FSR)[24-25]可表示为

$$W_{\mathrm{FWHM\ VIPA}}=\frac{\lambda_0^2}{2\pi n_{\mathrm{e}} t\cos(\theta_{\mathrm{in}})}\frac{1-Rr}{\sqrt{Rr}},\tag{1}$$

$$R_{\mathrm{FSR\ VIPA}}=\frac{\lambda_0^2}{2n_{\mathrm{e}} t\cos(\theta_{\mathrm{in}})},\tag{2}$$

式中：R、r、t、n_{e}和θ_{i}分别是VIPA元件前表面反射系数、后表面反射系数、厚度、折射率和倾斜角；λ_0是中心波长；$\theta_{\mathrm{in}}=\theta_{\mathrm{i}}/n_{\mathrm{e}}$是折射角。在中心波长一定时，其光谱分辨率主要取决于厚度和前后表面反射系数，光谱检测范围主要取决于厚度。

宽带平行光经柱面镜线聚焦在VIPA元件入射窗口，在竖直方向上形成级次重叠的色散光。随后，衍射光栅在水平方向分离该色散光的重叠级次，形成的二维(2D)色散光被成像镜聚焦在面阵探测器表面。探测面上光谱分布如图1(b)所示。竖直方向受VIPA元件的色散作用，波长λ_0(圆点)代表VIPA元件的不同干涉级次。水平方向，光栅将VIPA元件的重叠级次分离形成倾斜的条纹。通过特征波长λ_0可识别光谱图像中VIPA元件的单个FSR，将条纹从左到右、从下到上依次连接即可获得一维光谱[21]。交叉色散型VIPA光谱仪的光谱检测范围主要取决于光栅和面阵探测器水平方向的尺寸，光谱分辨率则取决于VIPA色散元件。

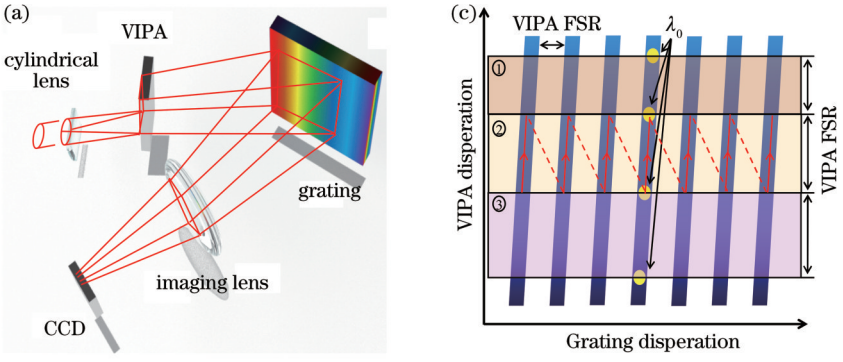

图1　VIPA光谱仪示意图。(a)结构示意图；(b)二维光谱图像示意图

Fig. 1　Schematic diagram of VIPA spectrometer. (a) Structure diagram; (b) schematic diagram of 2D spectral image

2.2　光谱反演原理

根据Beer-Lambert定律，气体吸收系数$\alpha(v)$、透过光强$I_{\mathrm{t}}(v)$及入射光强$I_0(v)$[26-27]满足以下关系

$$\alpha(v)=-\ln\left[I_{\mathrm{t}}(v)/I_0(v)\right]/L=\frac{\chi N_{\mathrm{L}} P T_{\mathrm{ref}}}{P_0 T}Sg(v),\tag{3}$$

式中：χ为气体摩尔分数；P为气体压力；T为气体温度；L为有效吸收光程；S为吸收线强；$N_{\mathrm{L}}=2.6869\times10^{19}$ molecule/cm^{3}为参考温度$T_{\mathrm{ref}}=273.15$ K和参考压力$P_0=1$ atm(1 atm=1.01×10^5 Pa)条件下的洛施米德常数；$g(v)$为分子吸收线型。本文使用Voigt函数表示$g(v)$[26]，公式为

$$g_{\mathrm{V}}(v)=g_{\mathrm{V}}(v_0)\times\left[(1-x)\exp\left(-0.693y^2\right)+\frac{x}{1+y^2}+g_{xy}\right],\tag{4}$$

$$g_{xy}=0.016\times(1-x)\times\left[x\left[\exp\left(-0.0841y^{2.25}\right)-\frac{1}{1+0.0210y^{2.25}}\right]\right],\tag{5}$$

$$g_{\mathrm{V}}(v_0)=\frac{1}{2\Delta v_{\mathrm{V}}\left(1.065+0.447x+0.058x^2\right)},\tag{6}$$

式中：v_0为谱线的中心波长；$x=\Delta v_{\mathrm{L}}/\Delta v_{\mathrm{V}}$；$y=|v-v_0|/\Delta v_{\mathrm{V}}$；$\Delta v_{\mathrm{V}}$为Voigt线型的半峰半宽(HWHM)，可表示为$0.5346\Delta v_{\mathrm{L}}+\left(0.2166\Delta v_{\mathrm{L}}^2+\Delta v_{\mathrm{D}}^2\right)^{0.5}$；$\Delta v_{\mathrm{D}}$和$\Delta v_{\mathrm{L}}$分别是Gauss线型展宽和Lorentz线型展宽[26]。

$$\Delta v_{\mathrm{D}}=3.581\times10^7 v_0\sqrt{T/M},\tag{7}$$

$$\Delta v_{\mathrm{L}}=\left[\chi\gamma_{\mathrm{self}}+(1-\chi)\gamma_{\mathrm{air}}\right]P_{\mathrm{p}}\left(\frac{T_0}{T}\right)^n,\tag{8}$$

式中：M为待测气体相对分子质量；γ_{self}为气体自展宽

系数；γ_{air}为空气展宽系数；P_p为探测气体分压；n为温度依赖系数；T_0=296 K。

在仪器探测中，受限于光谱仪的分辨率，探测光强可视为透过光强与仪器函数的卷积[23,27]，展宽后的吸收系数$\alpha_{ILS}(v)$满足以下关系

$$\alpha_{ILS}(v)\cdot L=-\ln\left[\frac{I_t(v)\otimes\phi(v)}{I_0(v)\otimes\phi(v)}\right]=-\ln\left[T(v)\otimes\phi(v)\right],\tag{9}$$

式中：$T(v)$为理论透过光强，可通过$\exp\left[-\alpha(v)\cdot L\right]$得到；$\phi(v)$为VIPA光谱仪的仪器函数，其半峰全宽等于光谱仪分辨率[1,23]，其线型为面积归一化的Lorentz函数[1,18,25]。

通过式(3)～(9)可建立分子浓度、光谱仪光谱分辨率与实测吸收光谱之间的联系。使用最优化算法可准确反演仪器的性能、分子各项参数等。如文献[27]中根据HITRAN数据库计算出以气体摩尔分数χ为自变量的理论吸收系数$\alpha_{ILS}(\chi)$，进而通过最小二乘拟合计算得到气体摩尔分数χ，表示为

$$\chi=\underset{x\geqslant 0}{\arg\min}\left[-\ln\left(\frac{I-I_d}{I_0-I_d}\right)-\alpha_{ILS}(\chi)\cdot L\right]^2,\tag{10}$$

式中：I为实测吸收光谱；I_0为背景光谱；I_d为暗背景；arg min算符表示目标函数取最小值时的变量值。

3　实验装置

宽带CO_2吸收光谱检测装置如图2所示，主要由超连续光源、光学吸收多通池和VIPA光谱仪等组成。宽带激光由单模光纤出射，经光纤准直器(PAF2P-A4B，Thorlabs，美国)形成束腰半径为1 mm的平行光束，经滤光片选取检测1.42～1.45 μm波长范围用于探测研究。随后出射光在气体吸收池内部多次反射后经光纤耦合器耦合进单模光纤，最终连接至VIPA光谱仪的光纤接口以实现光谱采集。

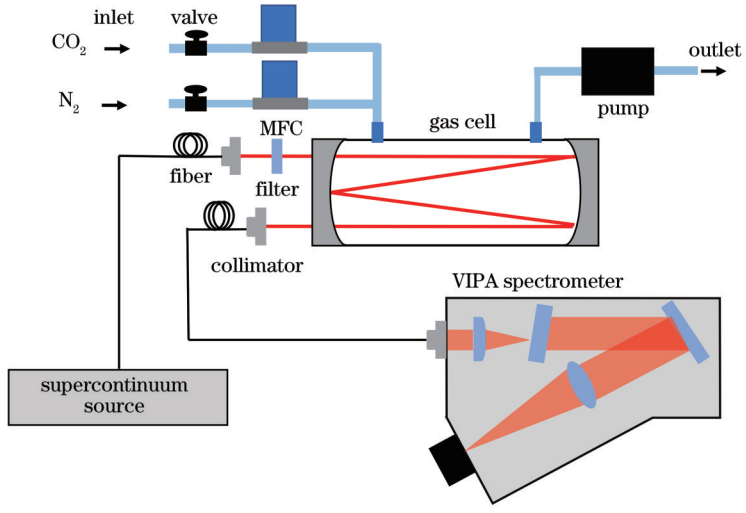

图2　宽带CO_2吸收光谱测量装置示意图

Fig. 2　Schematic diagram of broadband CO_2 absorption spectrum measurement device

实验探测光源为超连续光源(SC-5，YSL Optics，武汉)，其平均功率为0.9 mW/nm，波长覆盖范围为0.47～2.4 μm。光学吸收多通池为研制的Chernin型光学多通池。池体由5片曲率半径为0.5 m的凹面反射镜组成，基长为0.5 m，池体内光束的最大反射次数可达128次(即最大64 m有效光程)。由于本文测试气体为纯CO_2，为获得强度合适的CO_2吸收信息以及避免吸收饱和，调节池体反射次数为8，该条件下吸收池的有效吸收光程约为4 m。VIPA光谱仪的所有光学元件均安装在长宽高为40 cm×28 cm×12 cm的一体化硬铝箱体中。在调节结构上：将柱面镜与光纤准直器的调节装置结合，通过光纤准直器与柱面镜的相对位置关系调节入射光轴方向，达到减小光谱仪离轴像差的目的；删减了成像透镜和面阵相机的调节结构，使装置更为精简；添加了光栅旋转结构，扩展了光谱仪的实际可检测范围(取决于VIPA元件镀膜范围)。其中：光纤准直器的焦距为15 mm，光纤出射光经准直器后形成光束半径为3.6 mm的平行光束；柱面镜(CY108114，LBTEK，深圳)的焦距为100 mm；VIPA元件(OP-6721-1686-7，LightMachinery，美国)自由光谱范围为60 GHz，基底材料为熔融石英，厚度为1.68 mm，尺寸为22 mm×24 mm(长×宽)，其中入射窗口区大小为22 mm×3 mm(长×宽)，各表面镀膜的有效范围为1.26～1.50 μm，VIPA元件的倾斜角约为5°；全息闪耀光栅(GH25-24V，Thorlabs，加拿大)的刻线密度为1200 line/mm，尺寸为25 mm×25 mm；成像透镜(MAD518-C，LBTEK，深圳)焦距为200 mm；面阵探测器(LD-SW640，Leading Optoelectronic，西安)位于成像镜的焦平面上，光敏面尺寸为640×512，像素大小为20 μm。

在光谱测量时分别通入高纯N_2和高纯CO_2气体，待腔内压力稳定在200 mbar后采集背景光谱图像I_0和信号光谱图像I。池内气压通过阀控以及质量流量控制器（MFC）控制，压力值由真空规（CDG-500，Agilent，美国）监控。

4 结果与讨论

4.1 一维光谱提取

VIPA光谱仪使用15 ms曝光时间、1 frame/s的采集速度进行光谱测量。图3(a)、(b)分别为测量高纯N_2（纯度99.999%）得到的背景光谱图像I_0和测量高纯CO_2（纯度99.999%）得到的吸收光谱图像I，其中图3(b)中条纹变暗是CO_2分子的吸收所致。图3(c)为直方图均衡化算法处理后的吸收图像，其中背景归一化的吸收可通过$-\ln\left[(I-I_d)/(I_0-I_d)\right]$得到，$I_d$为暗背景图像。使用直方图均衡化算法[28]可增强吸收图像的吸收特征，提升弱吸收峰与背景的对比度，便于以图像的纵向周期性结构分辨VIPA光谱仪图像的自由光谱范围。图3(c)中光斑代表信号增强后的CO_2吸收峰，由CO_2吸收在纵向的周期性分布可知，面阵探测器共检测到VIPA元件的三个自由光谱区范围，方框标记的光斑为CO_2气体在6961.9901 cm^{-1}处的吸收，根据该吸收可准确标定出如实线标识的一个自由光谱区范围。

在一维光谱反演时，每个条纹的相对强度根据该条纹中心在水平方向上5 pixel（取决于条纹宽度）的平均值得到，每个像素对应的波长根据测量的吸收峰位置与HITRAN数据库中的位置进行标定。如图3(d)所示，像素位置与波长呈三次多项式关系[12]，拟合不确定度小于1%。

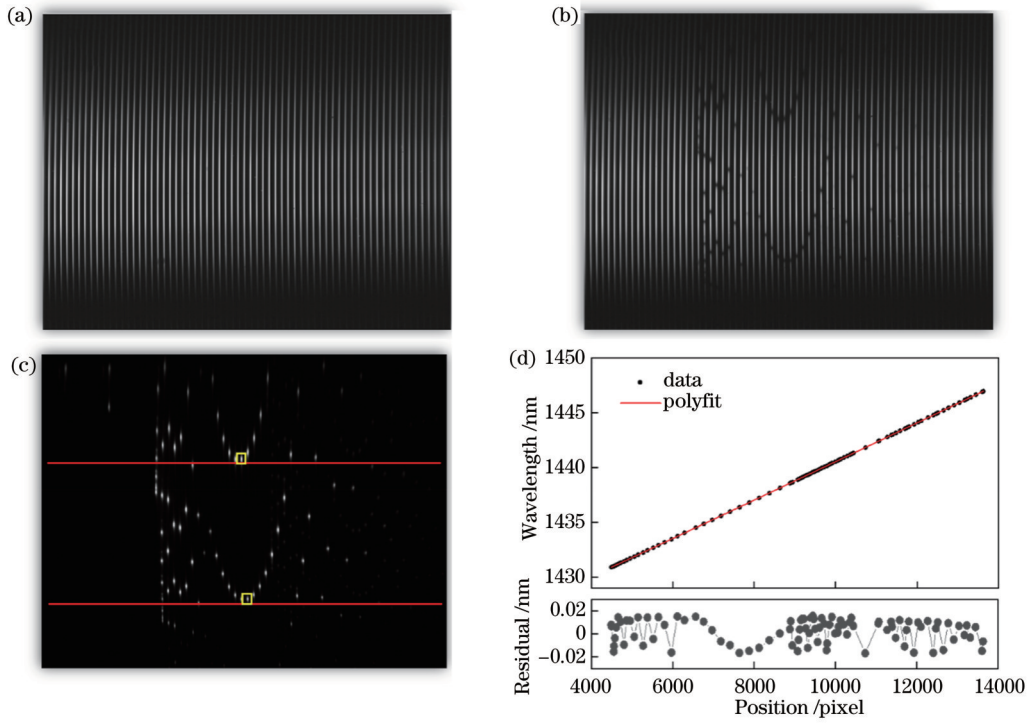

图3 光谱反演流程。(a)纯N_2光谱图像；(b)纯CO_2光谱图像；(c)CO_2吸收图像；(d)光谱标定示意图

Fig. 3 Flow of spectral inversion. (a) Pure N_2 spectral image; (b) pure CO_2 spectral image;(c) pure CO_2 absorption image; (d) schematic diagram of spectral calibration

4.2 光谱分辨率

VIPA光谱仪的实际光谱分辨率通过高纯CO_2的孤立吸收峰来评估。图4(a)为200 mbar、298 K条件下高纯CO_2气体在6971.0021 cm^{-1}处的理论吸收光谱，其Voigt半峰全宽为0.049 cm^{-1}。以仪器函数的半峰全宽为自变量，根据式(3)～(9)，以0.001 cm^{-1}为迭代步长，在0.01～0.04 cm^{-1}区间内将仪器函数与CO_2的理论透射光谱进行卷积，计算理论吸收与实测CO_2吸收的均方根误差，得到最小残差条件下的半峰全宽为0.024 cm^{-1}（4.5 pm）。图4(b)为CO_2的理论吸收光谱和受仪器展宽后的吸收光谱。使用实测CO_2吸收光谱对仪器函数进行验证，结果如图4(c)所示，残差（SD）为3×10^{-3}，证明仪器函数反演准确。表1展示了已报道的部分近红外VIPA光谱仪，从光谱分辨率来看，本装置处于领先水平。

4.3 CO_2宽带吸收光谱拟合

通过1.43～1.45 μm CO_2实测吸收光谱与理论吸收光谱的对比，研究了光谱反演算法与VIPA光谱仪应用于宽光谱、高分辨测量的准确性。CO_2气体的单个吸收峰可通过式(3)～(9)计算得到，由于实验采用

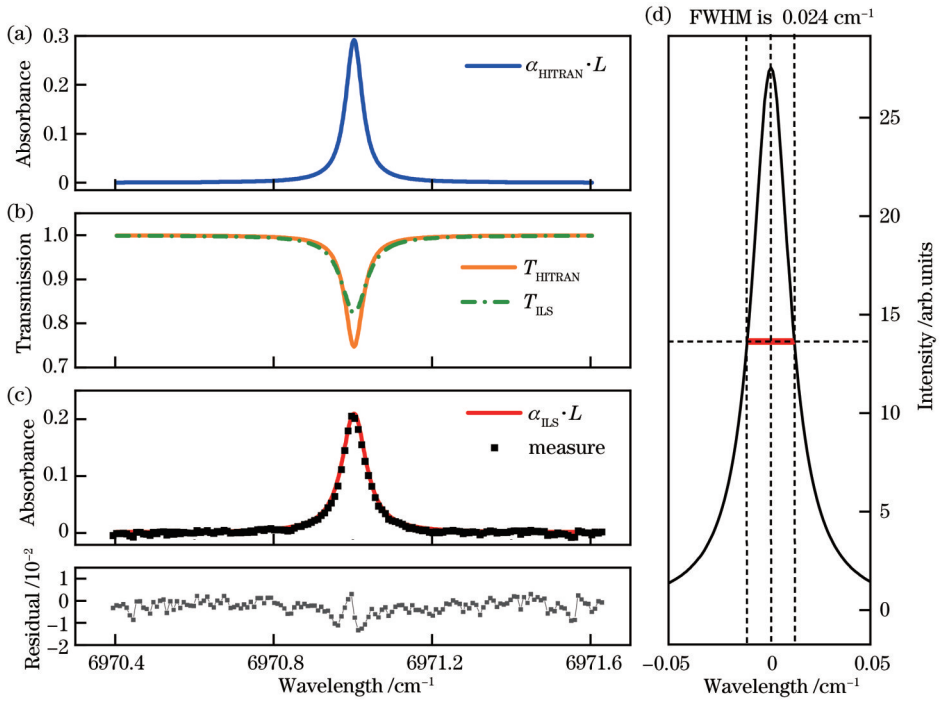

图 4　仪器函数反演示意图。(a)纯 CO_2 气体理论吸收谱；(b)纯 CO_2 理论透射谱和展宽的理论透射谱；(c)纯 CO_2 实测吸收、理论吸收及残差图；(d)仪器函数图

Fig. 4　Schematic diagram of instrument lineshape function inversion. (a) Theoretical absorption of pure CO_2; (b) pure CO_2 theoretical and broadened theoretical transmission spectra; (c) measured absorption, theoretical absorption, and residual data of pure CO_2; (d) photograph of instrument lineshape function

表 1　部分近红外 VIPA 光谱仪性能对比表

Table 1　Performance comparison of near-infrared VIPA spectrometers

Year	Center wavelength / μm	Spectral resolution / pm	Spectral coverage / nm	Reference
2008	1.60	6.9	25	[1]
2015	1.57	4.9	15	[29]
2016	2.00	26.9	40	[3]
2016	1.55	8.0	23	[30]
2017	1.45	4.8	20	[31]
2018	1.58	12.6	20	[32]
2020	1.60	4.6	25	[33]
2023	1.45	4.5	25	Proposed

高纯 CO_2 作为测试气体，因此仅考虑自展宽系数。计算 HITRAN 数据库中对应波段 CO_2 气体的每个吸收峰后，通过逐线积分的方式得到宽带理论吸收光谱 $\sum_{1}^{n}\alpha_{ILS}(v)\cdot L$[26]，其中 n 为对应波段的理论吸收峰个数。图 5(a)展示了 6900～6990 cm^{-1} 波段实测吸收谱与 200 mbar、298 K 条件下纯 CO_2 的理论吸收光谱。图中每个数据点代表一个像素，实线为逐线积分的叠加结果。图 5(b)和图 5(c)分别展示了 6942～6948 cm^{-1} 波段和 6970～6976 cm^{-1} 波段的局部拟合结果，其中柱图为实际检测到的 CO_2 吸收峰位置及对应线强。从理论吸收峰分布可以看出，图 5(b)代表谱线重叠区域，图 5(c)代表谱线分立区，光谱数据拟合残差的来源主要是分子展宽模型的缺陷，Voigt 线型未考虑 Dicke 收敛效应或速度依赖的碰撞展宽效应[34-36]，在高分辨率、高频率精度的吸收光谱拟合时会导致“W”形残差的出现且残差大小与吸收峰值相关[37]。实际探测的 129 个 CO_2 吸收峰与理论吸收的峰形、峰值均较为符合，全谱最小拟合残差为 5.31×10^{-3}，证明研制的 VIPA 光谱仪可用于实际气体的宽带、高分辨光谱测量。系统的最小可探测吸收可利用无吸收处基线的标准偏差来评估[38]。图 5(a)中基线波动的标准偏差为 2.68×10^{-3}，最强吸收峰对应的 CO_2 分子探测极限为 9.10×10^{15} molecule/cm^3，对应的体积分数为 1.85×10^{-3}，该指标可通过增加光程进一步改进。

5　结　　论

本文搭建了一台一体化结构的近红外 VIPA 光谱仪，单帧谱宽约为 25 nm(140 cm^{-1})，光谱分辨率为 4.5 pm(0.024 cm^{-1})。在装置设计方面，通过添加光栅旋转结构，将光谱仪的检测范围扩展为 1.26～1.50 μm，通过改进光谱仪的调节结构，在精简装置的同时降低了系统的离轴像差。在光谱提取算法方面，通过添加图像增强算法提升弱信号的提取精度。在光谱反演算法方面，考虑了光谱仪的仪器展宽，提升了气体参数反演的准确度。最后结合超连续光源与

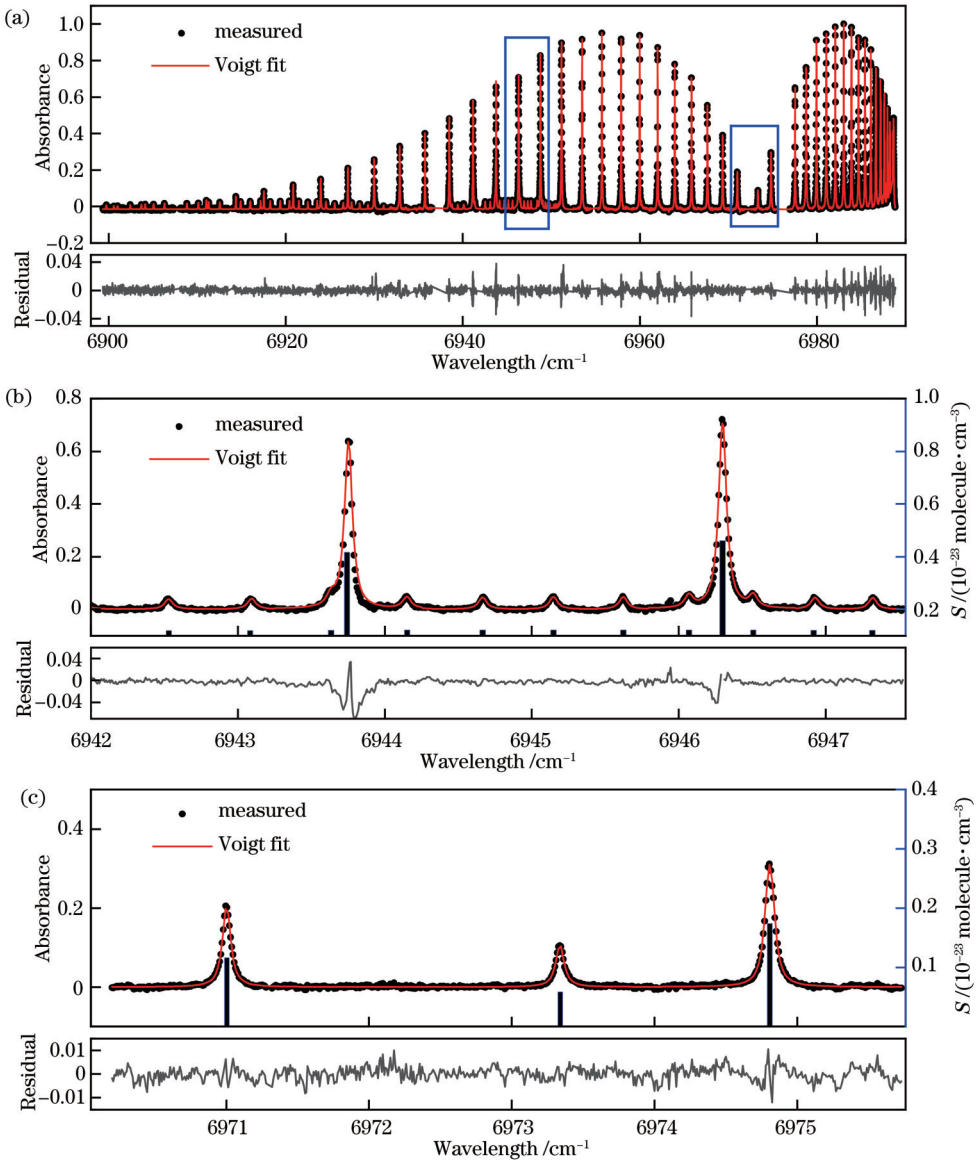

图 5 CO_2吸收光谱图。(a) 200 mbar、298 K 条件下 6900～7000 cm^{-1}纯 CO_2实测光谱、逐线积分理论谱及残差;(b)6943～6948 cm^{-1}局部拟合图;(c) 6970～6976 cm^{-1}局部拟合图

Fig. 5 Photograph of CO_2 absorption spectrum. (a) Measured spectrum, line-by-line integrated simulated spectrum, and residual error from 6900 cm^{-1} to 7000 cm^{-1} of pure CO_2 at the pressure of 200 mbar and 298 K conditions; (b) partial fitting results for the 6943-6948 cm^{-1} band; (c) partial fitting results for the 6970-6976 cm^{-1} band

Chernin 型光学多通池,检测了 1.43～1.45 μm 波段 CO_2吸收光谱。通过 1.435 μm(6971.0021 cm^{-1})处 CO_2的单个实测吸收峰的拟合结果验证了光谱仪的实测光谱分辨率。将该反演算法应用于多峰拟合,通过对比实测光谱区域内测量吸收谱与理论吸收谱,验证了 VIPA 光谱仪应用于宽带、高分辨气体吸收光谱测量的准确性与可靠性。未来结合光腔可实现痕量气体的宽带、高分辨光谱测量[39-40]。

参 考 文 献

[1] Thorpe M J, Balslev-Clausen D, Kirchner M S, et al. Cavity-enhanced optical frequency comb spectroscopy: application to human breath analysis[J]. Optics Express, 2008, 16(4): 2387-2397.

[2] Zhao W X, Fang B, Lin X X, et al. Superconducting-magnet-based faraday rotation spectrometer for real time *in situ* measurement of OH radicals at 10^6 molecule/cm^3 level in an atmospheric simulation chamber[J]. Analytical Chemistry, 2018, 90(6): 3958-3964.

[3] Klose A, Ycas G, Cruz F C, et al. Rapid, broadband spectroscopic temperature measurement of CO_2 using VIPA spectroscopy[J]. Applied Physics B, 2016, 122(4): 78.

[4] 刘栋沅,方波,赵卫雄,等.基于磁旋转光谱技术的氧气传感器研究[J/OL].光学学报:1-16[2023-05-02].http://kns.cnki.net/kcms/detail/31.1252.o4.20230509.1409.172.html.
Liu D Y, Fang B, Zhao W X, et al. Oxygen sensor based on Faraday rotation spectroscopy[J/OL]. Acta Optica Sinica: 1-16 [2023-05-02]. http://kns.cnki.net/kcms/detail/31.1252.o4.20230509.1409.172.html.

[5] 许新玉,周家成,刘政等.基于高精度 PID 温控的宽带腔增强大气二氧化氮探测技术研究[J/OL].光学学报:1-20[2023-05-02].

http://kns. cnki. net/kcms/detail/31.1252.O4.20230509.1329.170.html.
Xu X Y, Zhou J C, Liu Z, et al. Research on broadband cavity enhanced atmospheric Nitrogen Dioxide detection technology based on high precision PID temperature control[J/OL]. Acta Optica Sinica: 1-20[2023-05-02]. http://kns. cnki. net/kcms/detail/31.1252.O4.20230509.1329.170.html.

[6] 曹章, 高欣, 陆方皞, 等. 激光吸收光谱层析成像及复杂燃烧场动态监测[J]. 中国激光, 2022, 49(19): 1904002.
Cao Z, Gao X, Lu F H, et al. Laser absorption spectroscopy tomography and dynamic monitoring of complex combustion field [J]. Chinese Journal of Lasers, 2022, 49(19): 1904002.

[7] Fang B, Zhao W X, Xu X Z, et al. Portable broadband cavity-enhanced spectrometer utilizing Kalman filtering: application to real-time, *in situ* monitoring of glyoxal and nitrogen dioxide[J]. Optics Express, 2017, 25(22): 26910-26922.

[8] Blanco M, Maspoch S, Villarroya I, et al. Geographical origin classification of petroleum crudes from near-infrared spectra of bitumens[J]. Applied Spectroscopy, 2001, 55(7): 834-839.

[9] Zhu X M, He J P. Numerical study of comb-based high-accuracy distance measurement utilizing VIPA interferometry[J]. Journal of Optics, 2019, 21(2): 025703.

[10] Wei N N, Fang B, Zhao W X, et al. Time-resolved laser-flash photolysis faraday rotation spectrometer: a new tool for total OH reactivity measurement and free radical kinetics research[J]. Analytical Chemistry, 2020, 92(6): 4334-4339.

[11] Zhao W X, Xu X Z, Fang B, et al. Development of an incoherent broad-band cavity-enhanced aerosol extinction spectrometer and its application to measurement of aerosol optical hygroscopicity[J]. Applied Optics, 2017, 56(11): E16-E22.

[12] Nugent-Glandorf L, Giorgetta F R, Diddams S A. Open-air, broad-bandwidth trace gas sensing with a mid-infrared optical frequency comb[J]. Applied Physics B, 2015, 119(2): 327-338.

[13] Alfano R R. The supercontinuum laser source[M]. New York: Springer-Verlag, 1989.

[14] Picqué N, Hänsch T W. Frequency comb spectroscopy[J]. Nature Photonics, 2019, 13(3): 146-157.

[15] Cossel K C, Waxman E M, Finneran I A, et al. Gas-phase broadband spectroscopy using active sources: progress, status, and applications[J]. Journal of the Optical Society of America B, 2016, 34(1): 104-129.

[16] Kawata S. Instrumentation for near-infrared spectroscopy[M]// Siesler H W, Ozaki Y, Kawata S, et al. Near-infrared spectroscopy. Weinheim: Wiley-VCH Verlag GmbH, 2007: 43-73.

[17] Keliher P N, Wohlers C C. Echelle grating spectrometers in analytical spectrometry[J]. Analytical Chemistry, 1976, 48(3): 333A-340A.

[18] Adler F, Thorpe M J, Cossel K C, et al. Cavity-enhanced direct frequency comb spectroscopy: technology and applications [J]. Annual Review of Analytical Chemistry, 2010, 3: 175-205.

[19] Shirasaki M. Large angular dispersion by a virtually imaged phased array and its application to a wavelength demultiplexer[J]. Optics Letters, 1996, 21(5): 366-368.

[20] Wang C A, Ding Z H, Mei S T, et al. Ultralong-range phase imaging with orthogonal dispersive spectral-domain optical coherence tomography[J]. Optics Letters, 2012, 37(21): 4555-4557.

[21] Diddams S A, Hollberg L, Mbele V. Molecular fingerprinting with the resolved modes of a femtosecond laser frequency comb [J]. Nature, 2007, 445(7128): 627-630.

[22] Bjork B J, Bui T Q, Heckl O H, et al. Direct frequency comb measurement of OD + CO → DOCO kinetics[J]. Science, 2016, 354(6311): 444-448.

[23] Bailey D M, Zhao G, Fleisher A J. Precision spectroscopy of nitrous oxide isotopocules with a cross-dispersed spectrometer and a mid-infrared frequency comb[J]. Analytical Chemistry, 2020, 92(20): 13759-13766.

[24] Xiao S J, Weiner A M. An eight-channel hyperfine wavelength demultiplexer using a virtually imaged phased-array (VIPA)[J]. IEEE Photonics Technology Letters, 2005, 17(2): 372-374.

[25] Xiao S J, Weiner A M, Lin C. A dispersion law for virtually-imaged phased-array spectral dispersers based on paraxial-wave theory[J]. IEEE Journal of Quantum Electronics, 2004, 40(4): 420-426.

[26] Chen W D, Yi H M, Wu T, et al. Photonic sensing of reactive atmospheric species[M]. Chichester: John Wiley & Sons, 2017: 4-6.

[27] 杨鑫宇, 彭志敏, 丁艳军, 等. 基于宽带紫外吸收的火焰温度和 OH/NH/NO 浓度同步测量[J]. 物理学报, 2022, 71(17): 173301.
Yang X Y, Peng Z M, Ding Y J, et al. Synchronous measurement of flame temperature and OH/NH/NO concentration based on broadband ultraviolet absorption[J]. Acta Physica Sinica, 2022, 71(17): 173301.

[28] 章毓晋. 图像工程[M]. 4 版. 北京: 清华大学出版社, 2018: 73-75.
Zhang Y J. Image engineering[M]. 4th ed. Beijing: Tsinghua University Press, 2018: 73-75.

[29] Kowzan G, Paradowska M, Zaborowski M, et al. Broadband CO_2 measurements with VIPA spectrometer in the near-infrared [J]. Photonics Letters of Poland, 2015, 7(3): 78-80.

[30] Scholten S K, Anstie J D, Hébert N B, et al. Complex direct comb spectroscopy with a virtually imaged phased array[J]. Optics Letters, 2016, 41(6): 1277-1280.

[31] Hänsel A, Reyes-Reyes A, Persijn S T, et al. Temperature measurement using frequency comb absorption spectroscopy of CO_2[J]. Review of Scientific Instruments, 2017, 88(5): 053113.

[32] Yang L J, Li Y, Wei H Y. High-precision gas refractometer by comb-mode-resolved spectral interferometry[J]. Scientific Reports, 2018, 8: 16447.

[33] Karim F, Scholten S K, Perrella C, et al. Ultrahigh-resolution direct-frequency-comb spectrometer[J]. Physical Review Applied, 2020, 14(2): 024087.

[34] Goldenstein C S, Hanson R K. Diode-laser measurements of linestrength and temperature-dependent lineshape parameters for H_2O transitions near 1.4 μm using Voigt, Rautian, Galatry, and speed-dependent Voigt profiles[J]. Journal of Quantitative Spectroscopy and Radiative Transfer, 2015, 152: 127-139.

[35] Schreier F. Computational aspects of speed-dependent Voigt profiles[J]. Journal of Quantitative Spectroscopy and Radiative Transfer, 2017, 187: 44-53.

[36] 郑健捷, 朱文越, 刘强, 等. 1 μm 波段水分子吸收光谱双光程同步测量方法研究[J]. 物理学报, 2021, 70(16): 163301.
Zheng J J, Zhu W Y, Liu Q, et al. Study on dual-optical paths for simultaneous measurement method of water vapor absorption spectrum in 1 μm band[J]. Acta Physica Sinica, 2021, 70(16): 163301.

[37] 王振, 杜艳君, 丁艳军, 等. 基于傅里叶变换的波长扫描腔衰荡光谱[J]. 物理学报, 2019, 68(20): 204204.
Wang Z, Du Y J, Ding Y J, et al. Wavelength-scanned cavity ring down spectroscopy based on Fourier transform[J]. Acta Physica Sinica, 2019, 68(20): 204204.

[38] 杨娜娜, 方波, 王春晖, 等. 中红外波长调制离轴积分腔输出光谱技术应用于 OH 自由基高灵敏度探测研究[J]. 光子学报, 2023, 52(3): 0352123.
Yang N N, Fang B, Wang C H, et al. Wavelength modulation off-axis integrated cavity output spectroscopy for high-sensitivity detection of OH radicals in mid-infrared[J]. Acta Photonica Sinica, 2023, 52(3): 0352123.

[39] Roberts F C, Lewandowski H J, Hobson B F, et al. A rapid, spatially dispersive frequency comb spectrograph aimed at gas phase chemical reaction kinetics[J]. Molecular Physics, 2020,

118(16): 1733116.
[40] Fleisher A J, Bjork B J, Bui T Q, et al. Mid-infrared time-resolved frequency comb spectroscopy of transient free radicals [J]. The Journal of Physical Chemistry Letters, 2014, 5(13): 2241-2246.

High-Resolution and Broadband Spectral Measurement of CO_2 Based on Virtually Imaged Phased Array Spectrometer

Zhou Hao[1,2], Zhao Weixiong[1,2*], Lü Bingxuan[1,2], Cui Weihua[1], Fang Bo[1], Yang Nana[1], Zhang Weijun[1,2]

[1]*Anhui Institute of Optics and Fine Mechanics, Hefei Institutes of Physical Sciences, Chinese Academy of Sciences, Hefei* 230031, *Anhui, China*;

[2]*University of Science and Technology of China, Hefei* 230026, *Anhui, China*

Abstract

Objective Broadband and high-resolution spectroscopy plays a significant role in many research fields such as atmospheric trace gas detection, industrial monitoring, precision measurement, and basic physics and chemistry. Large spectral bandwidth allows for the simultaneous detection of multiple species, which enables a single instrument to have many functions. However, detection techniques that can provide a pm-level spectral resolution over a wide bandwidth still need to be further studied. The virtually imaged phased array (VIPA) is a plane-parallel etalon, where the input beam is injected at an angle through an entrance window on the front face. The multiple reflections occur within the VIPA etalon. The emerging light interferes to make different frequencies exit at different angles. VIPA spectrometer is an orthogonal dispersion system composed of VIPA and grating and can achieve spectral coverage of tens of nm in a single frame and spectral resolution of pm. In the past years, the VIPA spectrometer has been widely applied in high-precision broadband spectral measurement. However, practical applications of VIPA spectrometer face the following problems. First, some algorithms that employ gas absorption to calibrate the VIPA spectrometer ignore the instrument lineshape function (ILS), and second, these algorithms are difficult to calibrate when weakly absorbed. Additionally, the adjustment structure of the VIPA spectrometer can still be improved. Our paper reports an improved near-infrared spectrometer based on the VIPA and presents the experimental details and performance evaluation. The broadband and high-resolution measurement technology of CO_2 in 1.43-1.45 μm is carried out by combining the supercontinuum source and multi-pass cell. The results verify the reliability of the system and the accuracy of the improved data processing algorithm.

Methods The experimental system mainly consists of a supercontinuum laser, a Chernin muti-pass cell, and a VIPA spectrometer. The broadband light is collimated by the aspheric collimator. Then the emergent light is reflected eight times inside the gas cell and finally connects to the interface of the VIPA spectrometer by a single-mode fiber to acquire the CO_2 absorption spectrum. The experimental source is a supercontinuum laser with a spectral coverage of 0.47-2.4 μm. The Chernin cell is composed of five pieces of plano-concave mirrors with a radius of 0.5 m. To obtain CO_2 absorption of appropriate intensity and avoid absorption saturation, the mirror angle of the Chernin cell is adjusted to realize the reflection number of 8 and the optical path of 4 m. The VIPA spectrometer is made of high-strength hard aluminum alloy with dimensions of 400 mm×280 mm×120 mm. The main improvements of the spectrometer structure are as follows. The adjusting structure of the cylindrical lens and the collimator is combined to change the incident optical axis, and the off-axis aberrations of the VIPA spectrometer are reduced. The adjusting structure of the imaging lens is improved and the CCD leads to more compact spectrometer. Meanwhile, the grating rotation structure is added and the spectral coverage of the VIPA spectrometer is extended. The system employs pure N_2 absorption as the background image (I_0) and pure CO_2 absorption as the signal image (I). The algorithm subtracts the dark image from each of the signal and background images and then adopts Eq. (10) to subtract the baseline to get the absorption image. Finally, the algorithm extracts the one-dimensional spectra according to the rules shown in Fig. 2 and realizes the absorption spectral inversion.

Results and Discussions The fitting residual of the CO_2 absorption spectrum at 6971.0021 cm^{-1} is 3×10^{-3} [Fig. 4(c)], which verifies the correctness of the improved algorithm with the spectral resolution of the VIPA spectrometer being 4.5 pm [Fig. 4(d)]. By generalizing unimodal fitting to multimodal fitting, the broadband theoretical absorption spectrum can be obtained by line-by-line integration [Fig. 5(a)]. The minimum fitting residual of the whole spectrum (1.43-

1.45 μm) is 5.31×10^{-1}, proving that the developed VIPA spectrometer can be utilized for broadband and high-resolution spectral measurement of gases. The standard deviation (SD) of the baseline is 2.68×10^{-1} [Fig. 5(a)], and the detection limit of CO_2 molecules corresponding to the highest absorption peak of line intensity is 1.85×10^{-1}, which can be improved by increasing the optical path.

Conclusions A high-resolution near-infrared VIPA spectrometer with a relatively simple structure, a spectral resolution of 4.5 pm, and a spectral coverage of 25 nm in a single frame is developed. Improving the adjustment structure of the VIPA spectrometer makes the spectrometer more compact, reduces the off-axis aberrations, and extends the actual spectral coverage of the VIPA spectrometer. In terms of the data processing algorithm, the extraction accuracy of weak signals is improved by adding image enhancement algorithms, and the accuracy of gas parameter inversion is improved by considering the ILS. Finally, the broadband and high-resolution measurement technology of CO_2 in 1.43-1.45 μm is carried out by combining the supercontinuum source and multi-pass cell. The fitting results of the single absorption peak at 6971.0021 cm^{-1} verify the spectral resolution of the VIPA spectrometer. The accuracy and reliability of the VIPA spectrometer applied to the measurement of broadband and high-resolution gas absorption spectrum are verified by comparing the measured absorption spectrum with the theoretical absorption spectrum. In the future, the VIPA spectrometer combined with optical cavity can realize broadband and high-resolution spectral measurement of trace gases.

Key words virtually imaged phased array spectrometer; broadband absorption spectroscopy; high resolution; CO_2 detection